GLOBAL JOURNAL OF PURE AND APPLIED SCIENCES VOL. 10, NO. 4, SEPTEMBER 2004: 595 - 605
COPYRIGHT(C) BACHUDO SCIENCE CO. LTD. PRINTED IN NIGERIA. ISSN 1118-0579

AN IMPROVED MODELLING OF ASYNCHRONOUS MACHINE WITH SKIN-EFFECT.

O. I. OKORO

(Received 24 March, 2004; Revision Accepted 19 July, 2004)

ABSTRACT

The conventional method of analysis of Asynchronous machine fails to give accurate results especially when the machine is operated under high rotor frequency. At high rotor frequency, skin-effect dominates causing the rotor impedance to be frequency dependant. This paper therefore presents an improved method of modelling skin-effect in asynchronous machine under dynamic condition. The computed results are compared with the conventional model. The differences in the comparison underscore the need for the proposed model.

KEYWORDS: Conventional method, Skin-effect, Rotor impedance, Asynchronous machine, Simulation.

INTRODUCTION

The conventional method of analysis has been applied by several researchers to model the dynamic behaviour of Asynchronous machine(Jordan 1967, Krause 1965, Jordan 1965). This method of analysis has been proved to be inadequate for application involving high rotor frequency and for application requiring the operation of the machine above its rated voltage(Smith 1996, He and Lipo 1984). Under dynamic conditions, the lower section of the rotor bar experiences a higher inductance than the upper section of the rotor bar due to non-uniform flux distribution, thereby causing the current to flow primarily in the upper portion of the bar. This phenomenon of decrease in inductance and increase in resistance of rotor conductors is known as the deep-bar effect or the skin-effect(Liwschitz-Garik 1955, Alger 1995). Therefore, in modelling the Asynchronous machine for skin effect, accurate modelling of the rotor bar becomes imperative. In(Okoro 2002), the lumped-parameter method has been used to model the rectangular rotor bar. In the said work, the rotor bar was divided into five sections. In[(Okoro 2003), the lumped-parameter method was also applied but extended by dividing the rotor bar into six sections. The paper permits the impedance of a rectangular rotor bar to be computed with minimal error when compared with the actual rotor bar impedance. The error in the analysis is shown in Figure 1. The results in (Okoro 2003) have been used to carry out the present study since the error involved is less than that of Okoro(Okoro 2002).

The paper first models the Asynchronous machine using the conventional model. The skin-effect model is then presented together with the mechanical model that completely describes the machine's performances in dynamic states. Lastly, the method of simulation and the obtained results are presented and discussed.

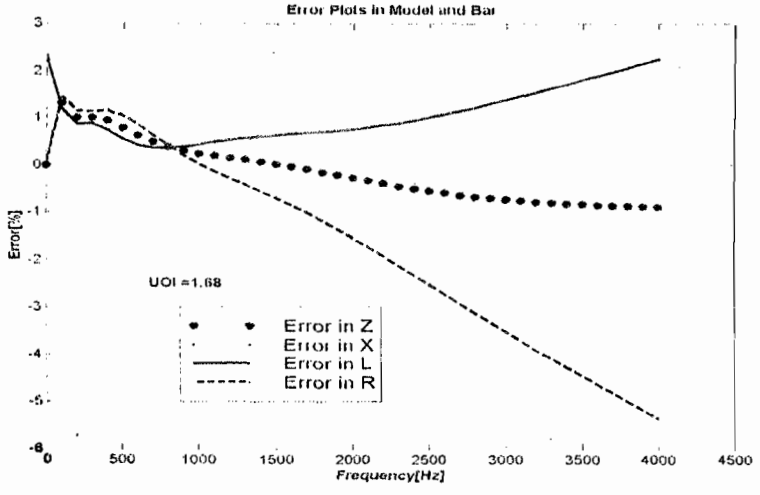

Figure 1: Error in the 6-section rotor bar model(Okoro 2003).

CONVENTIONAL MODEL

The conventional model of the machine is achieved by making the following assumptions:

(i) The machine is symmetrical with a linear air-gap and magnetic circuit.
(ii) Saturation effect is neglected

O. I. OKORO, Department of Electrical Engineering, University of Nigeria, Nsukka - Nigeria

(iii) Skin-effect and temperature effect are neglected
(iv) Harmonic content of the mmf wave is neglected
(v) The stator voltages are balanced.

he non-linear differential equations which describe the dynamic performance of an ideal symmetrical Asynchronous iachine can be represented in state variable form as:

$$\dot{\mathbf{i}} = -[\mathbf{L}]^{-1}([\mathbf{R}] + \omega_r[\mathbf{G}])[\mathbf{i}] + [\mathbf{L}]^{-1}[\mathbf{V}] \quad (1)$$

:quation(1) represents the electrical model of the machine and in rotor reference frame, the parameters in equation(1) ecome(Okoro 2002),

$$[\mathbf{V}] = [V_{qs} \quad V_{ds} \quad 0 \quad 0]^t \quad (2)$$

$$[\mathbf{R}] = \begin{bmatrix} R_s & 0 & 0 & 0 \\ 0 & R_s & 0 & 0 \\ 0 & 0 & R_r & 0 \\ 0 & 0 & 0 & R_r \end{bmatrix} \quad (3)$$

$$[\mathbf{L}] = \begin{bmatrix} L_s & 0 & L_m & 0 \\ 0 & L_s & 0 & L_m \\ L_m & 0 & L_r & 0 \\ 0 & L_m & 0 & L_r \end{bmatrix} \quad (4)$$

$$[\mathbf{G}] = \begin{bmatrix} 0 & L_s & 0 & L_m \\ -L_s & 0 & -L_m & 0 \\ 0 & 0 & 0 & 0 \\ 0 & 0 & 0 & 0 \end{bmatrix} \quad (5)$$

$$[\mathbf{i}] = [i_{qs} \quad i_{ds} \quad i_{qr} \quad i_{dr}]^t \quad (6)$$

Where,

$$L_s = L_{ls} + L_m \quad (7)$$

$$L_r = L_{lr} + L_m \quad (8)$$

Jnder balanced condition, the stator voltages of a three-phase Asynchronous machine may be considered as sinusoidal and expressed as

$$V_{as} = \sqrt{2}V\cos\omega_b t \quad (9)$$

$$V_{bs} = \sqrt{2}V\cos\left(\omega_b t - \frac{2\pi}{3}\right) \quad (10)$$

$$V_{cs} = \sqrt{2}V\cos\left(\omega_b t + \frac{2\pi}{3}\right) \quad (11)$$

These stator voltages are related to the d-q frame of reference by(Krause 1965)

$$\begin{bmatrix} V_{qs} \\ V_{ds} \end{bmatrix} = [C]\begin{bmatrix} V_{as} \\ V_{bs} \\ V_{cs} \end{bmatrix} \quad (12)$$

Where,

$$[C]=\frac{2}{3}\begin{bmatrix}\cos\theta & \cos\left(\theta-\frac{2\pi}{3}\right) & \cos\left(\theta-\frac{4\pi}{3}\right)\\ \sin\theta & \sin\left(\theta-\frac{2\pi}{3}\right) & \sin\left(\theta-\frac{4\pi}{3}\right)\end{bmatrix} \quad (13)$$

By application of trigonometric identities(Stroud 1982), equation(13) can be further simplified to give,

$$V_{qs}=\sqrt{2}V\cos(\theta-\omega_b t) \quad (14)$$

$$V_{ds}=\sqrt{2}V\sin(\theta-\omega_b t) \quad (15)$$

In the same vein, the d-q axis stator currents are related to the three phase stator currents by

$$\begin{bmatrix}i_{qs}\\ i_{ds}\\ i_{os}\end{bmatrix}=\frac{2}{3}\begin{bmatrix}\cos\theta & \cos\left(\theta-\frac{2\pi}{3}\right) & \cos\left(\theta-\frac{4\pi}{3}\right)\\ \sin\theta & \sin\left(\theta-\frac{2\pi}{3}\right) & \sin\left(\theta-\frac{4\pi}{3}\right)\\ \frac{1}{2} & \frac{1}{2} & \frac{1}{2}\end{bmatrix}\begin{bmatrix}i_{as}\\ i_{bs}\\ i_{cs}\end{bmatrix} \quad (16)$$

The Electromagnetic torque, Te is given by (Krause 1986) as:

$$T_e=\frac{3}{2}PL_m\left(i_{qs}i_{dr}-i_{ds}i_{qr}\right) \quad (17)$$

where, P=Number of pole pairs and L_m = magnetizing inductance.

SKIN-EFFECT MODEL

In the modelling of the Asynchronous rotor bar for skin-effect, the lumped parameter method is used. A T-model network as shown in Figure 2a is used to model the rectangular rotor bar. The rotor bar of the machine is divided into six sections. The rotor bar resistance and inductance for each section are,

$$R_{sec}=\frac{L_s}{\chi_{cu}h_{sec}b_{Nut}} \quad (18)$$

$$L_{sec}=\frac{\mu_o L_s h_{sec}}{b_{Nut}} \quad (19)$$

where,

μ_o = Permeability of free space, b_{Nut} = Width of the rotor bar, L_s = length of rotor bar, χ_{cu} = conductivity of copper, h_{sec} = height of each section

It is important to note that equations(18) and (19) are modified to take account of all the bars and subsequently referred to the stator to give "Rr" and "Lr" as shown in the equivalent T-circuit of the Asynchronous machine, Figure 2b and Figure 2c.

The rotor parameters of Figure 2 are referred to the stator by using the transformation factor, k and the values defined mathematically by,

$$L1r=k^2L10\ ;\ L2r=k^2L2\ ;\ L3r=k^2L3;\ L4r=k^2L4 \quad (20a)$$

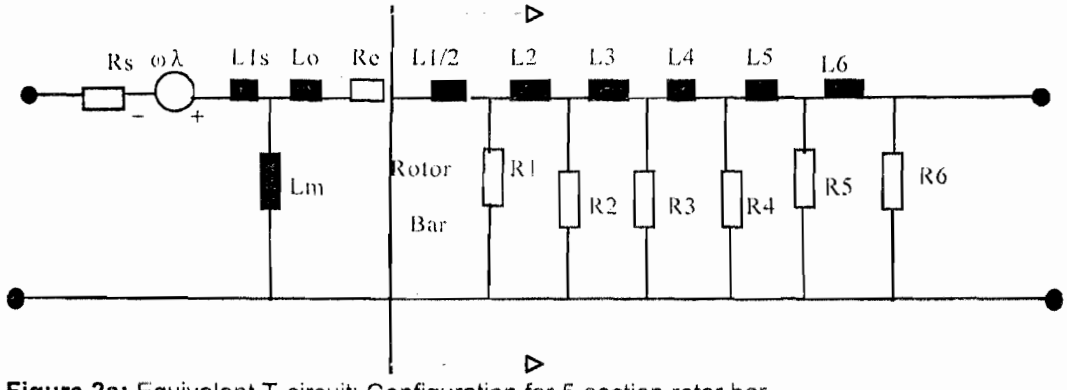

Figure 2a: Equivalent T-circuit; Configuration for 5-section rotor bar.

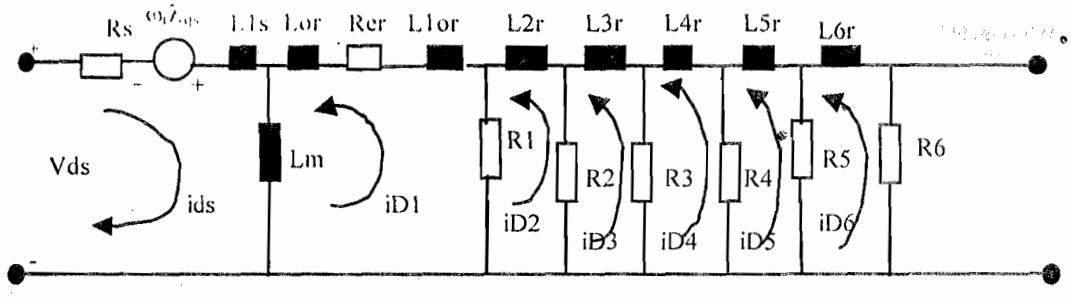

Figure 2b. Equivalent circuit for d-axis with rotor values referred to the stator.

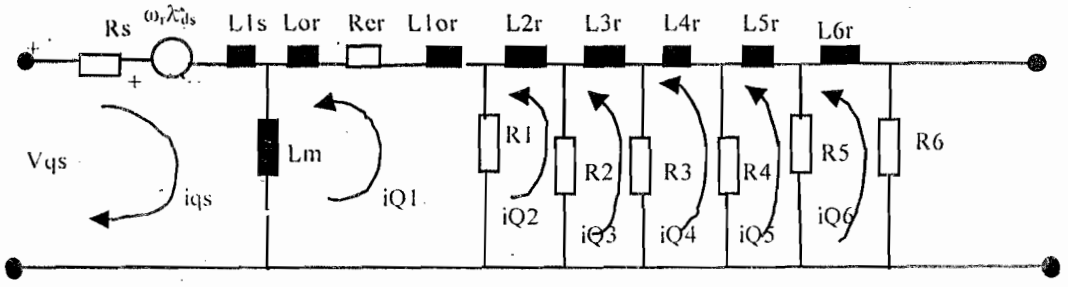

Figure 2c. Equivalent circuit for q-axis with rotor values referred to the stator.

$$L5r = k^2 L5\,;\ L6r = k^2 L6\,;\ \text{L10=Lor+L1or};\ \text{Re}\,r = k^2\,\text{Re}\,;\qquad R1r = k^2 R1 \tag{21b}$$

$$R2r = k^2 R2\,;\ R3r = k^2 R3\,;\ R4r = k^2 R4\,;\ R5r = k^2 R5\,;\ R6r = k^2 R6 \tag{21c}$$

where k_1 is defined thus(Nasar and Unnewehr 1979):

$$k_1^{\,2} = \frac{m1}{m2}\left(\frac{k_{w1}N1}{k_{w2}N2}\right)^2 \tag{22}$$

where,

m1 = number of phases on the stator; m2 = number of phases on the rotor; k_{w1} = stator winding factor; k_{w2} = rotor winding factor; N1 = number of series-connected turns per phase of the stator; N2 = number of series-connected turns per phase of the rotor.

But ,

m2 = (number of rotor bars)/(number of pairs of poles)

$$m2 = \frac{Q}{P} \tag{23}$$

Seinsch(Seinsch 1988) defines the relationship between the rotor bar resistance and the rotor resistance as:

$$R_2 = \frac{R_{bar}}{P} \tag{24}$$

with the equivalent rotor referred resistance as,

$$R'^{2} = k^{2} R_{bar} \tag{25}$$

where,

$$k^{2} = \frac{k_1^{\,2}}{P} \tag{26}$$

Table 1 shows the rotor circuit parameters at 4KHz rotor frequency extracted from (Okoro 2003) and used for the study of the dynamic behaviour of the test machine with skin-effect.

Table 1: Computed model impedance at 4KHz(Okoro 2003).

Resistance	[mΩ]	Inductance	[μH]
R_1	1.552	L_1	5.27e-2
R_2	0.924	L_2	7.06e-2
R_3	0.550	L_3	0.119
R_4	0.327	L_4	0.199
R_5	0.223	L_5	0.308
R_6	1.552	L_6	0.210

The machine d-q model equations are derived by taken the Kirchhoff's voltage expressions for each loop in Figure 2(Guiliemin 1953). In order to facilitate the digital computer simulation of the developed model, it is imperative to put the Kirchhoff's voltage equations in state variable form as in equation(2). By so doing, the following parameter identifications are made(Okoro 2002):

$$G = \begin{bmatrix} 0 & -Ls & 0 & -Lm & 0 & 0 & 0 & 0 & 0 & 0 & 0 & 0 & 0 & 0 \\ Ls & 0 & Lm & 0 & 0 & 0 & 0 & 0 & 0 & 0 & 0 & 0 & 0 & 0 \\ 0 & 0 & 0 & 0 & 0 & 0 & 0 & 0 & 0 & 0 & 0 & 0 & 0 & 0 \\ 0 & 0 & 0 & 0 & 0 & 0 & 0 & 0 & 0 & 0 & 0 & 0 & 0 & 0 \\ 0 & 0 & 0 & 0 & 0 & 0 & 0 & 0 & 0 & 0 & 0 & 0 & 0 & 0 \\ 0 & 0 & 0 & 0 & 0 & 0 & 0 & 0 & 0 & 0 & 0 & 0 & 0 & 0 \\ 0 & 0 & 0 & 0 & 0 & 0 & 0 & 0 & 0 & 0 & 0 & 0 & 0 & 0 \\ 0 & 0 & 0 & 0 & 0 & 0 & 0 & 0 & 0 & 0 & 0 & 0 & 0 & 0 \\ 0 & 0 & 0 & 0 & 0 & 0 & 0 & 0 & 0 & 0 & 0 & 0 & 0 & 0 \\ 0 & 0 & 0 & 0 & 0 & 0 & 0 & 0 & 0 & 0 & 0 & 0 & 0 & 0 \\ 0 & 0 & 0 & 0 & 0 & 0 & 0 & 0 & 0 & 0 & 0 & 0 & 0 & 0 \\ 0 & 0 & 0 & 0 & 0 & 0 & 0 & 0 & 0 & 0 & 0 & 0 & 0 & 0 \\ 0 & 0 & 0 & 0 & 0 & 0 & 0 & 0 & 0 & 0 & 0 & 0 & 0 & 0 \\ 0 & 0 & 0 & 0 & 0 & 0 & 0 & 0 & 0 & 0 & 0 & 0 & 0 & 0 \end{bmatrix} \quad (27)$$

$$[i] = [i_{ds} \quad i_{qs} \quad iD1 \quad iQ1 \quad iD2 \quad iQ2 \quad iD3 \quad iQ3 \quad iD4 \quad iQ4 \quad iD5 \quad iQ5 \quad iD6 \quad iQ6]^t \quad (28)$$

$$[V] = [Vds \quad Vqs \quad 0 \quad 0 \quad 0 \quad 0 \quad 0 \quad 0 \quad 0 \quad 0 \quad 0 \quad 0 \quad 0 \quad 0]^t \quad (29)$$

$$[R] = \begin{bmatrix} Rs & 0 & 0 & 0 & 0 & 0 & 0 & 0 & 0 & 0 & 0 & 0 & 0 & 0 \\ 0 & Rs & 0 & 0 & 0 & 0 & 0 & 0 & 0 & 0 & 0 & 0 & 0 & 0 \\ 0 & 0 & R11 & 0 & -R1r & 0 & 0 & 0 & 0 & 0 & 0 & 0 & 0 & 0 \\ 0 & 0 & 0 & R11 & 0 & -R1r & 0 & 0 & 0 & 0 & 0 & 0 & 0 & 0 \\ 0 & 0 & -R1r & 0 & R22 & 0 & -R2r & 0 & 0 & 0 & 0 & 0 & 0 & 0 \\ 0 & 0 & 0 & -R1r & 0 & R22 & 0 & -R2r & 0 & 0 & 0 & 0 & 0 & 0 \\ 0 & 0 & 0 & 0 & -R2r & 0 & R33 & 0 & -R3r & 0 & 0 & 0 & 0 & 0 \\ 0 & 0 & 0 & 0 & 0 & -R2r & 0 & R33 & 0 & -R3r & 0 & 0 & 0 & 0 \\ 0 & 0 & 0 & 0 & 0 & 0 & -R3r & 0 & R44 & 0 & -R4r & 0 & 0 & 0 \\ 0 & 0 & 0 & 0 & 0 & 0 & 0 & -R3r & 0 & R44 & 0 & -R4r & 0 & 0 \\ 0 & 0 & 0 & 0 & 0 & 0 & 0 & 0 & -R4r & 0 & R55 & 0 & -R5r & 0 \\ 0 & 0 & 0 & 0 & 0 & 0 & 0 & 0 & 0 & -R4r & 0 & R55 & 0 & -R5r \\ 0 & 0 & 0 & 0 & 0 & 0 & 0 & 0 & 0 & 0 & -R5r & 0 & R66 & 0 \\ 0 & 0 & 0 & 0 & 0 & 0 & 0 & 0 & 0 & 0 & 0 & -R5r & 0 & R66 \end{bmatrix} \quad (30)$$

Where,

$$R11 = \mathrm{Re}\,r + R1r;\ R22 = R1r + R2r;\ R33 = R2r + R3r;\ R44 = R3r + R4r \quad (31a)$$

$$R55 = R4r + R5r;\ R66 = R5r + R6r \quad (31b)$$

$$[L] = \begin{bmatrix} Ls & 0 & Lm & 0 & 0 & 0 & 0 & 0 & 0 & 0 & 0 & 0 & 0 & 0 \\ 0 & Ls & 0 & Lm & 0 & 0 & 0 & 0 & 0 & 0 & 0 & 0 & 0 & 0 \\ Lm & 0 & Lmr & 0 & 0 & 0 & 0 & 0 & 0 & 0 & 0 & 0 & 0 & 0 \\ 0 & Lm & 0 & Lmr & 0 & 0 & 0 & 0 & 0 & 0 & 0 & 0 & 0 & 0 \\ 0 & 0 & 0 & 0 & L2r & 0 & 0 & 0 & 0 & 0 & 0 & 0 & 0 & 0 \\ 0 & 0 & 0 & 0 & 0 & L2r & 0 & 0 & 0 & 0 & 0 & 0 & 0 & 0 \\ 0 & 0 & 0 & 0 & 0 & 0 & L3r & 0 & 0 & 0 & 0 & 0 & 0 & 0 \\ 0 & 0 & 0 & 0 & 0 & 0 & 0 & L3r & 0 & 0 & 0 & 0 & 0 & 0 \\ 0 & 0 & 0 & 0 & 0 & 0 & 0 & 0 & L4r & 0 & 0 & 0 & 0 & 0 \\ 0 & 0 & 0 & 0 & 0 & 0 & 0 & 0 & 0 & L4r & 0 & 0 & 0 & 0 \\ 0 & 0 & 0 & 0 & 0 & 0 & 0 & 0 & 0 & 0 & L5r & 0 & 0 & 0 \\ 0 & 0 & 0 & 0 & 0 & 0 & 0 & 0 & 0 & 0 & 0 & L5r & 0 & 0 \\ 0 & 0 & 0 & 0 & 0 & 0 & 0 & 0 & 0 & 0 & 0 & 0 & L6r & 0 \\ 0 & 0 & 0 & 0 & 0 & 0 & 0 & 0 & 0 & 0 & 0 & 0 & 0 & L6r \end{bmatrix} \quad (32)$$

Where,

$$Lmr = L\lambda r + Lm \quad (33)$$

MECHANICAL MODEL

Figure 3 represents the motor mechanical model schematic for the motor-load connection. The equation of motion of the motor and the coupling is given by

$$T_e - M_w = J_{m1}\frac{d^2\theta_m}{dt^2} \quad (34)$$

But,

$$\frac{d\omega_m}{dt} = \frac{d^2\theta_m}{dt^2} \quad (35)$$

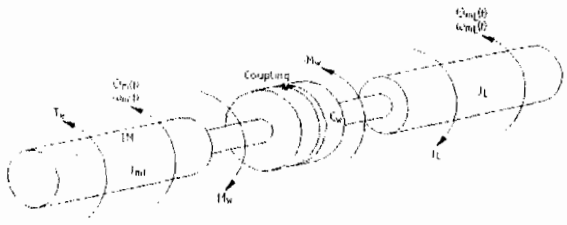

Figure 3: Motor mechanical model schematic with coupling.

Put equation(35) into equation(34), we have

$$T_e - M_w = J_{m1}\frac{d\omega_m}{dt} \quad (36)$$

Similarly, the equation of motion between the coupling and the driven load is related by

$$M_w - T_L = J_L\frac{d\omega_{mL}}{dt} \quad (37)$$

where,

$$\omega_{mL} = \frac{d\theta_{mL}}{dt} \quad (38)$$

By definition(Holzweißig and Dresig 1982),

$$M_w = c_w\left(\theta_m - \theta_{mL}\right) \quad (39)$$

Taking the first derivative of equation(39), equation(40) results,

$$\frac{dM_w}{dt} = c_w\left(\frac{d\theta_m}{dt} - \frac{d\theta_{mL}}{dt}\right) \quad (40)$$

Therefore, the general equation of the coupled system with damping factor(d_w) neglected can be expressed in matrix form as:

$$\begin{bmatrix}\dot{\omega}_m\\ \dot{\omega}_{mL}\\ \dot{M}_w\end{bmatrix} = \begin{bmatrix}0 & 0 & -\frac{1}{J_{m1}}\\ 0 & 0 & \frac{1}{J_L}\\ c_w & -c_w & 0\end{bmatrix}\begin{bmatrix}\omega_m\\ \omega_{mL}\\ M_w\end{bmatrix} + \begin{bmatrix}\frac{T_e}{J_{m1}}\\ -\frac{T_L}{J_L}\\ 0\end{bmatrix} \quad (41)$$

where,

J_{m1} = moment of inertia of induction motor; M_w = shaft torque; J_L = moment of inertia of the D.C. motor; c_w = stiffness constant of the shaft system; ω_{mL} = mechanical speed of the D.C. motor

The experimental determination of the shaft system stiffness constant, c_w has been reported by Okoro(Okoro 2002) to be 14320Nm/rad for the machine under test. The block diagram of equation(41) is shown in Figure 4.

EXPERIMENTATION AND COMPUTER SIMULATION RESULTS

The test machine is a KATT VDE 0530, Class F insulation, surfaced-cooled squirrel-cage Asynchronous motor. The rated power, speed, and current are 7.5KW, 1400rpm and 19.2A respectively. The test machine is a four-pole motor with 50Hz rated frequency and 340V rated voltage. Figure 5 shows the test machine. In order to determine the test machine parameters necessary to carry out the dynamic studies, several experiments were carried out. The No-load test was carried out at rated frequency and with balanced polypahse voltages applied to the stator terminals. Readings for the current, voltage, electrical power and speed were taken after the motor has been running for a considerable long period of time necessary for the bearings to be properly lubricated.

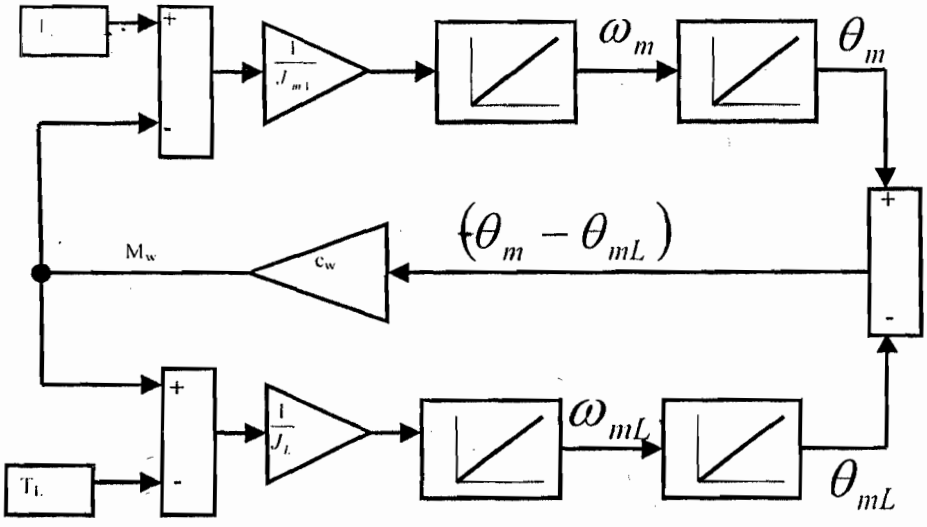

Figure 4. Block diagram of motor mechanical model with coupling.

Table 2: The machine data.

Output power	7.5KW
Rated voltage	340V
Winding connection	Delta
Number of poles	4
Rated speed	1400rpm
Rated frequency	50Hz
Stator resistance	2.52195Ω
Stator leakage reactance	1.95145Ω
Rotor resistance	0.976292Ω
Rotor leakage reactance	2.99451Ω
Magnetizing reactance	55.3431Ω
Rated current	19.2A
Estimated rotor inertia moment	0.117394Kgm^2

Blocked-rotor test and test with the injection of D.C. current in the stator windings were made at standstill. The retardation test was carried out at No-load with and without additional standard mass. The load test was carried out with constant load of 51.3Nm and frequency at a sinusoidal stator windings voltage.
The results of these experiments are recorded in Table 2 together with the name-plate data of the machine

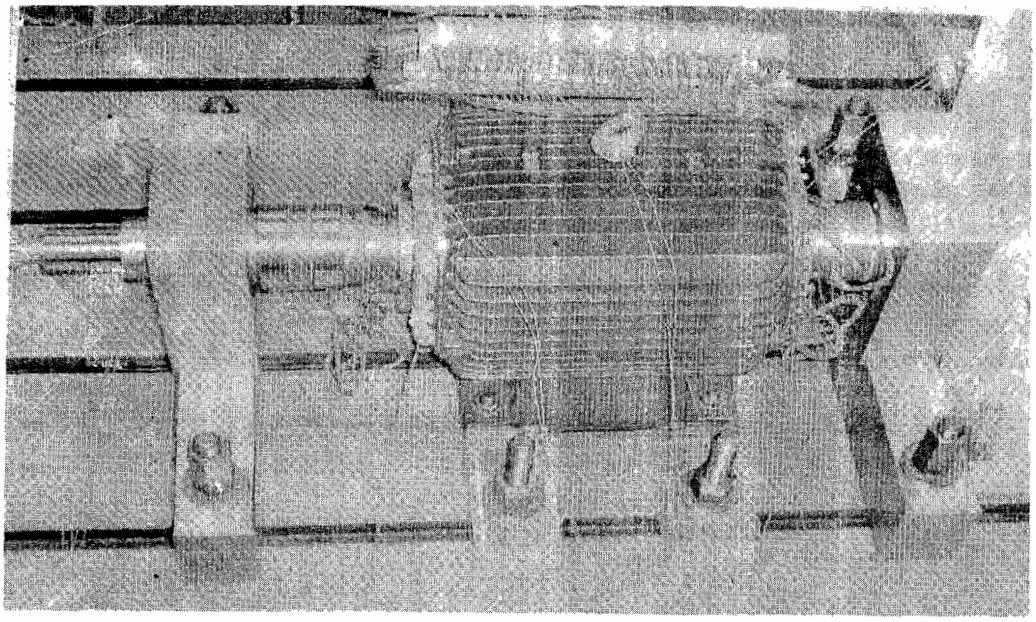

Figure 5. The 7.5KW test motor.

MATLAB function program which describes the differential equations of the machine models (Conventional and Skin-effect) in dynamic condition is developed and solved using the Fourth-order Runge-Kutta numerical method(The MATLAB 1997). Together with the mechanical model of the machine, the dynamic behaviour of the asynchronous machine at run-up can be simulated. The developed MATLAB m-files accept as input the test machine parameters in Table 2 and the rotor circuit parameters of Table 1 as in the case of skin-effect model. Figure 6 shows the time function of the mechanical rotor speed for the two models. It can be seen that the skin-effect model rises faster to synchronous speed than the conventional model.

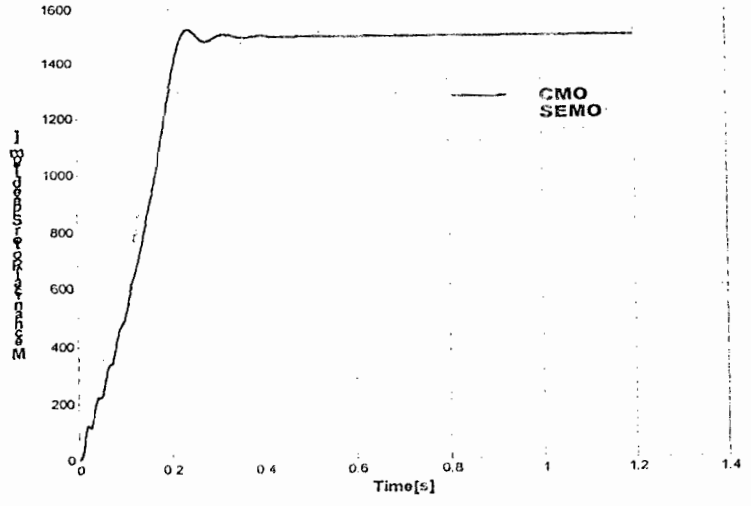

Figure 6. Graph of Mechanical rotor speed against Time.

The comparison between the conventional model and skin-effect model for the electromagnetic torque is depicted in Figure 7. At starting, the torque developed by the machine in the skin-effect machine model is about 20% higher than that of the conventional model.

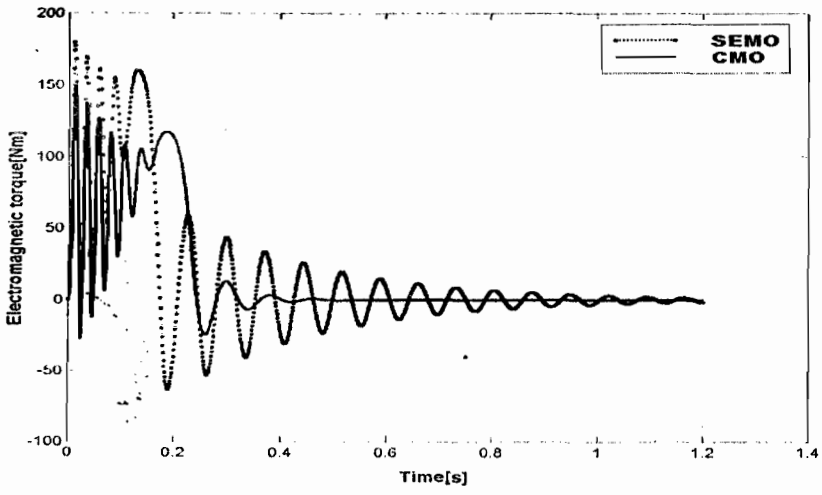

Figure 7: Graph of Electromagnetic torque against Time.

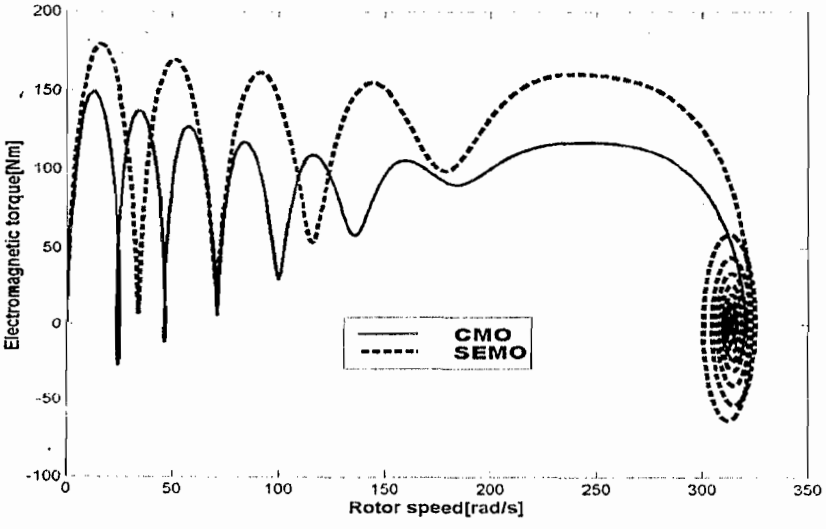

Figure 8: Graph of Electromagnetic torque against Rotor speed.

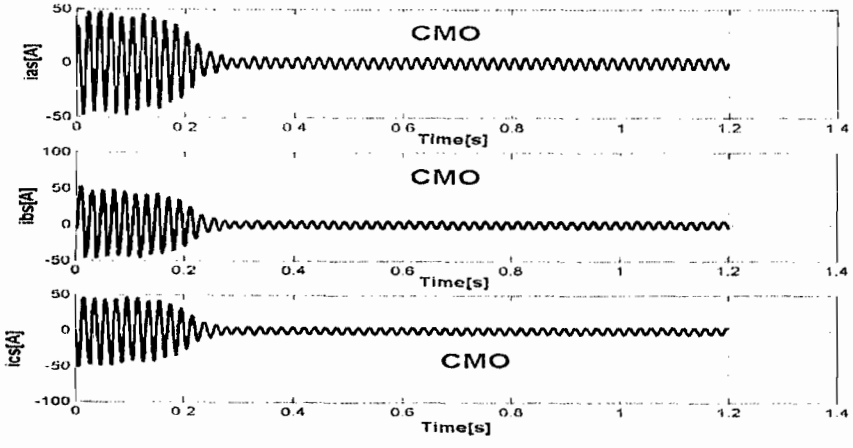

Figure 9. Graph of Stator phase currents against Time for the conventional model.

The same difference is observed in the graph of electromagnetic torque against rotor speed as shown in Figure 8. In the figure, the skin-effect model, shows higher peak torques for a given rotor speed than the conventional model. Figure 9 and Figure 10 show the time function of the stator phase currents for the conventional and skin-effect models respectively. Prolonged initial level of oscillations are observed in the phase currents of the conventional model.

Figure 10 shows higher initial starting current than that of Figure 9. The predicted time function of the bar currents in each rotor section show in Figure 11 indicates that the current magnitude decreases as the bar section increases.

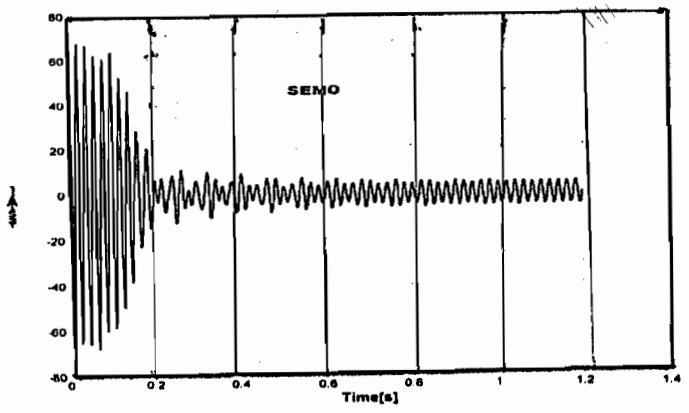

Figure 10a

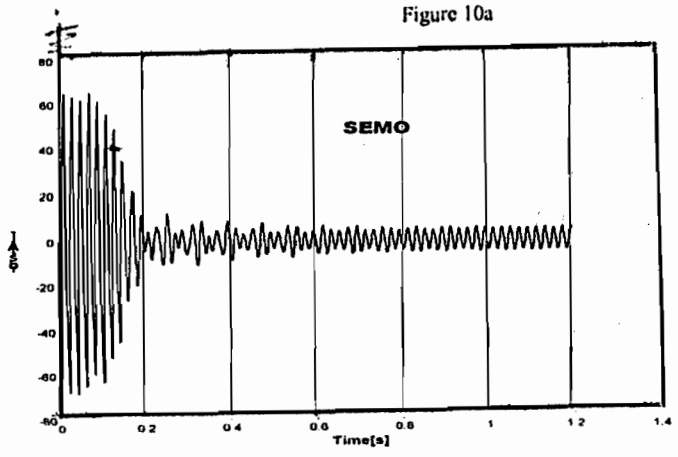

Figure 10b

Figure 10. Graph of Stator phase currents against Time for the skin-effect model.

CONCLUSION

The paper has presented an improved modelling of asynchronous machine with skin-effect. Comparison between the proposed skin-effect model and the conventional model under dynamic condition showed large errors in the predicted torque, speed and phase currents. Pertinently, for operation requiring high rotor frequency as in the case of PWM-operated asynchronous machine, the need for the proposed skin-effect model becomes highly imperative. By modelling for skin-effect in asynchronous machine, the time function of the stator phase currents, electromagnetic torque and the rotor mechanical speed at run-up condition can be predicted to the level that is close to the actual machine behaviour. However, inclusion of saturation effect can improve the accuracy of the predicted results considerably. Work in this direction is in progress and will soon be reported by the Author.

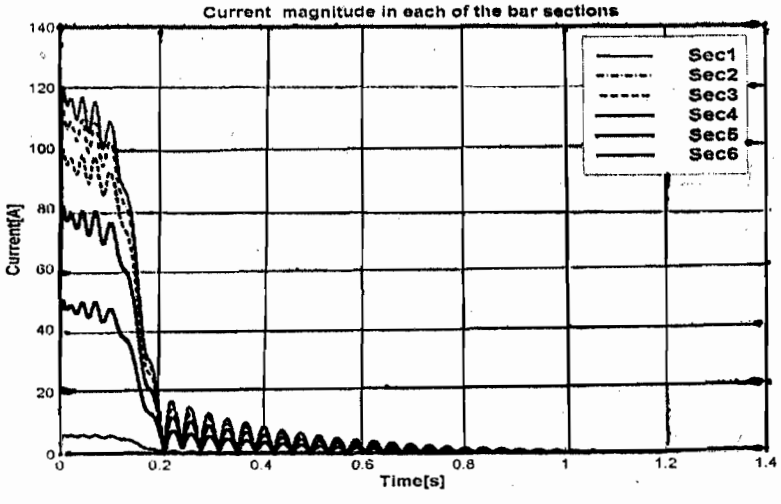

Figure 11: Graph of bar currents against Time .

ACKNOWLEDGEMENT

The author would like to thank Prof. Dr.-Ing. B. Weidemann for his useful discussion on the subject and to **DAAD** for her financial assistance during the research work at the University of Kassel, Germany.

REFERENCES

Alger, P. L., 1995. Induction machines: Their behaviour and uses. USA, Gordon and Brach Inc.

Guiliemin, E. A., 1953. Introductory circuit theory. New-York, Wiley.

He,Yi-Kang and Lipo, T. A., 1984. Computer simulation of an induction machine with spatially dependent saturation. IEEE Transaction on Power Apparatus and Systems, 4(103): 707 - 714.

Holzweißig, F. and Dresig, H., 1982. Lehrbuch der Maschinendynamik: maschinendynamische Probleme und ihre praktische Lösung. Zweite Auflage Springer-Verlag, Wien.

Jordan, H. E., 1967. Digital computer analysis of induction machines in dynamic systems. IEEE Transactions on Power Apparatus and systems, 6(86): 722 - 728.

Jordan, H. E., 1965. Analysis of induction machines in dynamic systems. IEEE Transaction on Power Apparatus and Systems, 11(84): 1080 - 1088.

Krause, P.C., 1986. Analysis of Electric Machinery. New York, McGraw-Hill.

Krause, P.C. and Thomas, C.H., 1965. Simulation of symmetrical induction machinery. IEEE Transaction on Power Apparatus and Systems, 11(84): 1038 - 1053.

Liwschitz-Garik, M. M., 1955. Computation of skin-effect in bars of squirrel-cage rotors. AIEE Transactions, 74 : 768-771.

Nasar, S. A. and Unnewehr, L. E., 1979. Electromechanics and Electric machines. New –York, John Willey and sons.

Okoro, O. I., 2002. Dynamic and Thermal modelling of Induction machine with non-linear effects. Doctor of Engineering Thesis, University of Kassel, Germany.

Okoro, O. I., 2003. An improved skin-effect model for a rectangular shaped rotor bar. Transaction NSE(Electrical Division), PP.46-52.

Seinsch, H. O., 1988. Grundlagen elektrischer Maschinen und Antriebe. Stuttgart, Teubner.

Smith, A. C., 1996. A transient induction motor model including saturation and deep bar effect. IEEE Transactions on Energy Conversion, 11(1): 8-15.

Stroud, K. A., 1982. Engineering Mathematics. Second Edition, London , Macmillan Press Ltd.

The MATLAB, 1997. The MATLAB Compiler User's guide, in Mathworks handbook. Math works.